Using representative time slices for optimization of thermal energy storage systems in low-temperature district heating systems

B. van der Heijde[a, b, c], L. Scapino[a, c, d], A. Vandermeulen[a, b, c], D. Patteeuw[a, b], R. Salenbien[a, c] and L. Helsen[a, b]

[a] EnergyVille, Genk, Belgium
[b] KU Leuven, Department of Mechanical Engineering, Leuven, Belgium
[c] VITO NV, Mol, Belgium
[d] Eindhoven University of Technology, Department of Mechanical Engineering, P.O. Box 513, 5600MB Eindhoven, The Netherlands

Abstract:

4th generation district heating and cooling networks (shortly THERNETs) are often coined as a crucial technology to enable the transition towards low-carbon smart energy systems. Most importantly, they open perspectives for integration of low-grade residual heat from industry, renewable energy sources (such as geothermal heat and cold and solar thermal collectors), more efficient energy conversion units (such as collective heat pumps), while thermal energy storage (TES) systems increase system flexibility.
In order to optimize design and control of such complex systems, a toolbox `modesto` (Multi-objective district energy systems toolbox for optimization) is under development. However, the representation of seasonal heat and cold storage systems on an annual basis requires large computational power. In an attempt to decrease computational cost, a technique with representative time slices (inspired by and combining aspects from optimization studies of electrical energy systems, unit commitment problems, thermal systems with short term energy storage and smaller scale industrial thermal systems with longer term energy storage) is developed and tested. The aim of this study is to investigate the applicability of such representative time periods to optimize seasonal TES systems in THERNETs. To this end a full year optimization is compared to one with representative time periods for a realistic case study that uses demand profiles from the city of Genk (Belgium) and energy system parameters from Marstal (Denmark).
This comparative study shows that modelling with representative periods is sufficient to mimic the behaviour of a full year optimization. However, when curtailment of solar heat injection occurs, not all representations yield the same results. It was found that for the studied case, a selection of 12 representative weeks performs best, while all reduced optimizations result in a substantial reduction (speed-up of on average x4.8 to x7.7) of the calculation time.

Keywords:

Thermal networks, Thermal energy storage, Seasonal storage, Optimization, Representative time slices, 4th generation district heating and cooling.

1. Introduction

In the transition to a sustainable and mainly renewable-based energy system, interest in energy storage in general, but more specifically thermal energy storage is increasing. The unpredictability and seasonal misalignment of different respective renewable energy sources and energy demand require the integration of energy storage systems to ensure security of supply. For optimal design of systems with seasonal thermal energy storage (STES) systems, it is necessary to use a representation of at least a full year period in order to take seasonal phenomena into account. Furthermore, sufficiently accurate models with a minimum time resolution are needed for meaningful results. `modesto` [1] is a linear optimization tool for the optimization of district energy systems, both from a design and a control perspective.

The combination of both a long time duration and a high time resolution leads to increasingly long calculation times. Because design optimization requires many optimizations to explore the design parameter space, a speed-up of computation is required.

Using representative days or time slices to represent a full year has already been established in electrical energy system modelling. Nahmmacher *et al.* [2] present an overview of how representative time periods are selected to account for demand fluctuations. However, they argue that these methods are not yet sufficiently able to account for variability at the production side, i.e. with the introduction of uncontrollable renewable energy sources. Their method is based on hierarchical clustering to select the most accurate representation of a full year.

Poncelet *et al.* [3] introduced a novel method to select representative time slices, namely an optimization based selection of representative periods. The objective of the optimization is to minimize deviation between duration curves[1] of the full year input profiles and their representation by means of representative time periods, where the number, number of repetitions and starting point of those representative time periods can be varied. In a basic version, only the duration curve of the original input profile is used, but additional duration curves can be introduced to include data variability (i.e. "ramping rates") or correlations between multiple input datasets. This method is compared against a number of other methods (random selection, hierarchic clustering and heuristic selection) and is shown to perform better when used in a reference optimization problem.

This methodology of representative time slices was used in combined design and control optimization of thermal systems by Patteeuw and Helsen [4]. They used the approach proposed by Poncelet to select six representative weeks, which is a compromise to limit the calculation time of the mixed integer linear programming (MILP) optimization problem. In this case, the full design optimization would be infeasible due to the size of the problem, so there is no information on how good the approximation is. However, it is shown that the duration curves of the representative input profiles approximate those of the original data accurately. The focus of Patteeuw and Helsen [4] is on residential systems with hot water buffers, whose thermal capacity only allows for daily or weekly storage. Hence, the representative weeks can be modelled with periodic boundary constraints on the state of the heat-storing elements. The study described in the current paper, however, considers seasonal energy storage effects and as a consequence these periodic boundary conditions cannot be applied.

Another example of thermal system optimization with representative time slices is the work of Timmerman *et al.* [5]. While they used a different method of representative time slice selection than Poncelet *et al.* (namely, the method of Welsch *et al.* [6]), they did incorporate electrical and thermal energy storage systems that act on a seasonal time-scale. They present an innovative method to account for the energy loss from these energy storage systems by using so-called *discount factors*. This paper only describes a simplified case to illustrate the effect of the use of representative time slices with an arbitrary time period selection. The results are not compared to a case with an equivalent full year optimization.

The current work combines the novel approaches of all of the above; Poncelet's time-slice selection method, Patteeuw's combination of control and design optimization and Timmerman's method to scale up to seasonal energy storage. The aim is to check whether the results of the time-slice optimization problem are actually representative for the full-year optimization of thermal energy storage systems in low-temperature district heating systems, as such a comparison appears to be absent in literature.

2. Methodology

This section guides the reader through methods used to select a number of representative periods, explains the reference case in which the full optimization and representative periods optimization are

[1] The **duration curve** of a time-varying profile shows the time duration during which a certain value of that profile is exceeded. The duration curve can be obtained by sorting the values of the time profile in a descending order. The best known duration curve is the yearly load duration curve (based on heat demand or electricity load), but any time-varying profile can be turned into a duration curve.

compared with its components and input data sources. Finally, the technique to connect state of charge of the storage tank between two representative time periods is explained.

2.1. Representative time period selection

The selection of representative time periods follows the approach of Poncelet *et al.* [3]: an optimization problem minimizes the deviation between the relevant duration curves of a full year and the 'upscaled representative time periods' duration curves (shortly called representative duration curves). In order to cast this problem into a MILP, the original duration curves are divided into 10 bins. Then, the optimizer selects a specified number of periods, all of which can be repeated for a certain number of times. The selection[2] and repetition[3] parameters are the optimization variables. Based on the number of repetitions and selection, a representative duration curve is constructed. The start and end time of each of the bins of the representative duration curve is compared to that of the original year and the deviation is minimized. The reader is referred to Poncelet et al. [3] for full details about the method. The objective function is the sum of the absolute errors of the end time of each of the bins for all of the duration curves considered. These errors can be weighted to put more or less emphasis on each of the curves.

In the current work, the representative periods need to be recombined into a year with a constant time step, as opposed to the method presented by Timmerman *et al.* [5]. Therefore, the scaling factor was restricted to an integer value (the period needs to be repeated a discrete number of times) and should be at least 1 for every selected period. If for instance representative weeks are selected, all scaling factors should add up to 52, leading to a year with 364 days instead of the usual 365 days, which means a scaling factor needs to be introduced (see Section 2.4) to compare the annual energy use.

A challenge in using any selection procedure based on duration curves is that chronology is lost; for seasonal energy storage systems, this chronology is essential. As an example, the selection algorithm could choose two consecutive weeks from a winter period, a single week from the first mid-season and a single week from summer; when they are scaled up and left in their original order, this will lead to a year starting with a long winter period, followed by a mid-season period and ending in a summer period. Comparing this to a normal year's seasonality, this representation is unacceptable.

In this paper, we propose a new method to recombine the selected time periods to a full year with a logical seasonality by first dividing the year into a number of seasons. In the presented results (see Fig. 3 in Section 3.1), four seasons are chosen, namely winter, spring mid-season, summer and autumn mid-season, based on the heat demand of the neighbourhood. The optimizer must select at least one representative period per season, and when the full year is reconstructed, the weeks are kept in original order.

In addition to the duration curves of the heat demand, solar heat generation and ambient temperature, also the correlation between the heat demand and the solar heat generation profiles is added. This profile is turned into an additional duration curve that makes sure that the general correlation between solar radiation and heat demand is respected, as described by Poncelet *et al.* [3].

2.2. Reference case, full year optimization and parameter sweep

For the sake of straightforward analysis, a very simple reference case is chosen, in which a single neighbourhood (inspired by a real neighbourhood in the city of Genk (Belgium)) is connected to an array of solar thermal collectors, a STES unit and a backup heating plant (see Fig. 1). Currently, all system components are connected to a single node and no heating network is considered, but this can

[2] **Selection:** optimization variable that indicates if a certain time period is selected (1) or not (0). A time period can start on every day of the year, and overlapping selections are not allowed.

[3] **Repetition:** for each selected period, this optimization variable indicates how often this time period should be repeated in the reconstruction of the full year time profile. When all repetitions of all selected time periods are combined, the combined duration should be that of the maximum integer number of such time periods that go in one year.

easily be extended. In order to have realistic values for a reference case, the energy system design parameters were chosen to emulate the solar district heating system of Marstal in Denmark [7], [8].

This reference system is optimized for a full year with a 1 h time step. The optimization problem calculates optimal control signals (heat flows to and from the storage tank and heat supplied by the backup boiler) for a full year, with the objective of minimal backup energy input. This can be related to the case where we want to minimize the use of fossil fuels and maximize the utilization of the solar thermal collectors. The state of the storage system is subject to a periodic boundary condition, i.e. the initial state on the 1st of January and the final state on the 31st of December are equal. All equations are linear and no integer optimization variables are considered in the reference case.

The reference system has a water storage volume of 100 000 m^3, 60 000 m^2 of solar thermal collectors and a backup heat generation plant with a nominal power of 3.85 MW, parameters which are inspired by the solar district heating system of Marstal (Denmark). The system is operated with a fixed supply temperature of 80°C and a return temperature of 40°C. As described before, the heat demand profile of the residential buildings is based on one of the selected neighbourhoods of Genk (Belgium), of which the annual heat demand amounts to 22.5 GWh, which is selected to reflect the heat load of Marstal.

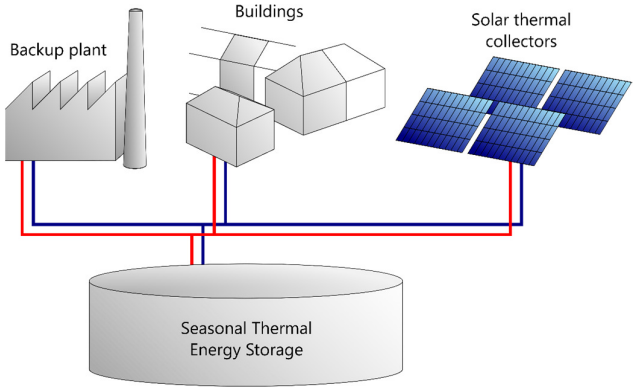

Fig. 1. Schematic representation of reference case.

2.3. Component models and input data

The models used in the reference case are all part of the `modesto` [1] Python package. This package relies on Pyomo [9] to compile optimization problems and currently uses optimization solver Gurobi [10], although Pyomo is compatible with a multitude of solvers. This section shortly describes these models and their assumptions, as well as the origin of the input data where relevant.

2.3.1. Energy storage system

The energy storage system is modelled according to Vandewalle and D'haeseleer [11], i.e. as a perfectly stratified tank with fixed high and low temperatures (T_H and T_L). The tank walls are thermally insulated, using insulation with constant thickness and thermal conductivity. Heat losses are calculated as pure conductive heat losses from the hot and cold tank volumes to the surroundings. Following the derivation of Vandewalle and D'haeseleer, the heat balance of the storage tank is written as:

$$Q_{stor}[n+1] = \zeta_H Q_{stor}[n] + \left(\dot{Q}_{ch}[n] - \dot{Q}_{loss,fix}[n]\right) \cdot \Delta t, \quad (1)$$

where $Q_{stor}[n]$ is the stored energy in the tank at time step n, $\dot{Q}_{ch}[n]$ is the heat flow charged into the tank and $\dot{Q}_{loss,fix}[n]$ is the state-independent heat loss from the tank during the same time step. ζ_H is a multiplication factor such that $1 - \zeta_H$ is the proportion of the stored energy lost during one time step. This factor accounts for the state-dependent heat losses. Beware of the fact that although the subscript *fix* is used, the state-independent heat losses do depend on the ambient temperature, whereas the state-dependent losses do not. The ambient temperatures are taken from a typical representative meteorological year in Uccle, Belgium (see IDEAS Modelica Library [12]).

No heat losses are associated to charging or discharging processes. The charging and discharging power are not constrained, although this is possible.

2.3.2. Solar thermal collectors

The solar thermal collector output is modelled using the ASHRAE93 test standard component from the Buildings Modelica Library (Wetter *et al.* [13]). In the model, typical meteorological data (including solar radiation) from Uccle, Belgium is used. A south-oriented collector with an area of 1 m^2 and inclined 40° with respect to the horizontal plane is taken as a reference. The solar profile was calculated for an input temperature of 40°C. The mass flow rate in the model has a constant value, but the pump is switched on or off depending on whether or not the incoming radiation is higher than the critical solar radiation.

In the optimization model, the heat generation profile derived in the previous paragraph is used as an input. As is the case for the storage model, fixed high and low temperatures are used. It is assumed that by varying the mass flow rate, a fixed temperature difference can be achieved with the same heat generation profile as the model described above. This approach was used because directly simulating a solar panel with a sophisticated (PID) control of the outlet temperature proved to increase the complexity significantly, without changing the annual heat production with more than 10% annually.

Normally, the optimizer will choose to use as much solar energy as possible because of its objective function. However, the optimizer has the option to curtail part of the solar thermal power when it cannot store it efficiently, usually due to insufficient storage capacity.

2.3.3. Heat demand from buildings

For the heat demand of the buildings, a number of neighbourhoods of interest have been selected in the city of Genk in Belgium. De Jaeger *et al.* [14] constructed building models based on geometrical data of all residential buildings in Genk. For simplicity, not all buildings have been simulated individually in this study. Instead, for every neighborhood three typical buildings are defined, as shown in Fig. 2: a detached, a semi-detached and a terraced building. Each of the three buildings is representative for all buildings of that type in the neighbourhood by averaging the dimensions and characteristics of the actual buildings, including wall and window surface, building materials, and insulation. The heat demand of the typical buildings is multiplied by the number of buildings of this type in the area.

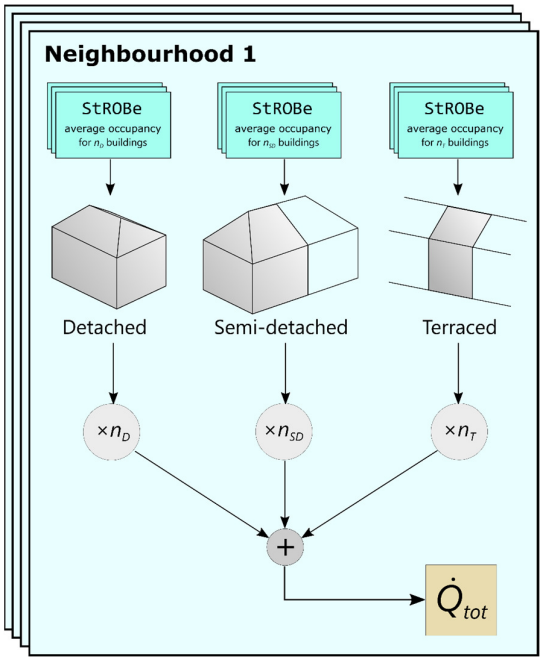

Fig. 2. Workflow for simulation of building heat demand.

The occupancy of the neighbourhoods is determined using the `StROBe` toolbox developed by Baetens and Saelens [15]. This toolbox uses statistical data for occupancy in residential buildings in Belgium and the Netherlands and samples electricity use, domestic hot water tapping and indoor temperature set-point profiles as realizations of these statistics. The input profile for each typical building is the average of *n* such profiles, where *n* stands for the number of buildings of that type as long as it does not surpass 50 (for memory considerations).

As described by the author [16], the resulting heat demand profiles were filtered (moving average) in order to correspond better to the demand variability expected from a district of this size. The average variability for district heating systems of various sizes was studied by Gadd and Werner [17].

2.3.4. Backup heat generation

The backup heater was simply modelled as an ideal heat source with the same fixed high and low temperatures as in all components before. The maximum heat output is limited to the nominal power level. Ramping rates could be limited as well, but this was omitted for the sake of simplicity.

2.4. STES optimization with representative weeks

To include STES into an optimization problem with representative time periods, the change in stored energy must be extrapolated from the single period that is optimized to all repetitions of that period.

However, energy storage goes hand in hand with some storage losses (see Section 2.3.1). These losses depend on:

- The current state of the storage tank,
- The temperature of the tank's surroundings and
- The design of the tank, i.e. insulation material and thickness, aspect ratio.

The losses need to be taken into account for the repetitions as well, hence it is not possible to just repeat the change in energy of the calculated period during all repetitions of that period. A higher energy content means higher losses and vice versa.

In order to achieve the coupling of subsequent representative time periods, Timmerman *et al.* [5] introduced a discount factor, an exact representation of energy losses under varying energy injections or extractions from the tank. This method is comparable to condensing systems with a linear state-space description, such that only the initial and final state variable remain.

In the current study, the time slices are equal in length and the number of time slice levels is limited to a single representative period with hourly time steps, whereas Timmerman uses more time slice levels (seasons, weeks, weekdays and weekend days, daily time brackets) and allows time slices of different lengths. However, implementing the problem as such led to very high compilation and solving times. Hence, a different approach was chosen: instead of only writing the state equations for the first repetition and extrapolating the change in stored energy, the state equations were implemented also during the other repetitions, while repeating the energy in- or output to the STES unit. This leads to a similar state transition equation as (1):

$$Q_{stor}[r, n+1] = \zeta_H Q_{stor}[r, n] + \left(\dot{Q}_{ch}[n] - \dot{Q}_{loss,fix}[n]\right) \cdot \Delta t \quad \forall r, n: n < n_f - 1, \tag{2}$$

$$Q_{stor}[r+1, n_0] = Q_{stor}[r, n_f], \tag{3}$$

where n_0 and n_f respectively are the initial and final time step of each repetition r of one of the representative periods. As (2) indicates, for each repetition the same sequence of heat interactions and state-independent losses is used. As such it is possible to benefit from the facts that all intermediate state variables are known and can easily be constrained to the extreme states of the storage tank, and that the heat losses are exact for the given inputs.

The optimization problem with representative periods (further called 'reduced optimization') has a number of additional constraints compared to the reference case: the storage state must be continuous

between two adjacent representative periods (see (3)). The energy content of the storage tank must be constrained between full and no charge. To this end, only the first and last repetition of every time slice need to be considered: since the (dis)charging time profile is the same during all of the repetitions, the minimum and maximum energy content for each of those time steps can only occur during the first and last repetition, as shown by Timmerman *et al.* [18].

The comparison takes into account that the representative year has a different number of days than a full year due to the integer number of repetitions of the representative time periods.

3. Results

The results are divided in two parts: Section 3.1 shows a summary of the reference case for the full year optimization as described in Section 2.1. Section 3.2 checks how well the optimization with representative periods represents the actual solution, thereby looking into some design parameter variations.

3.1. Example representative time period selection

Fig. 3 shows the results of a representative time profile for a selection of 12 weeks, compared to the original duration curves and time profiles. We see a very good approximation of the duration curves, while for the recombined year data, the overall trend is followed. The right graph in Fig. 3 shows that the recombined profile is slightly shifted in time. This is a result of the fact that the selection optimizer can cyclically "wrap around" the year while selecting, and the first week that is selected is mapped to the first week of the year. Since the optimization problem has a periodic boundary condition, this is not a problem.

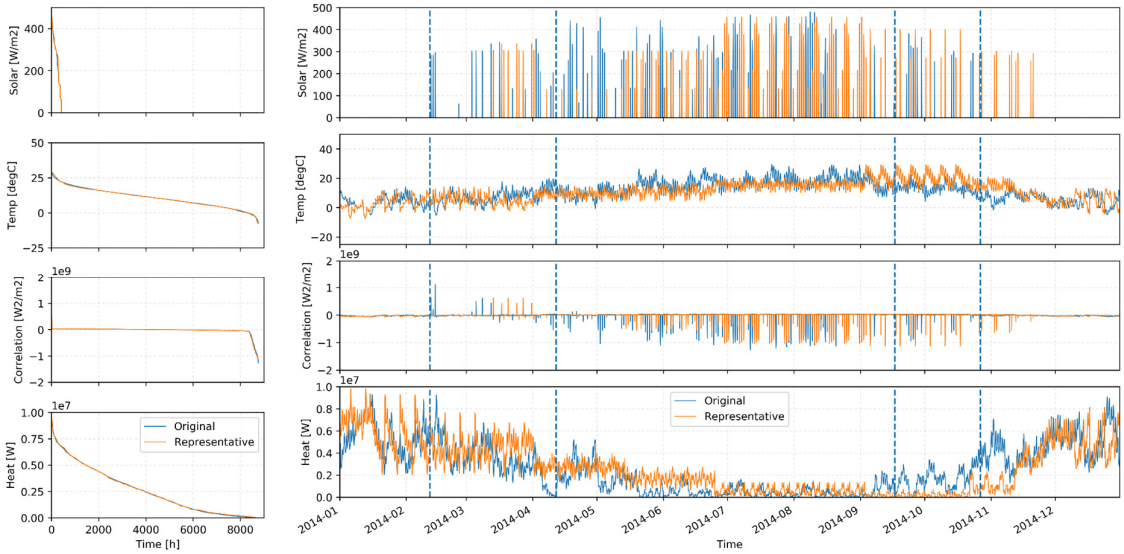

Fig. 3. Duration curves of unit area solar collector output, correlation between solar collector and heat demand profiles, ambient temperature and heat demand of the original profiles and representative time periods (left) and recombined time profiles compared to the original time series (right). These results are for a selection of 12 representative weeks. The dotted vertical lines in the right figure separate the seasons from which the start days of the representative time periods must be chosen. The first and last time brackets form one season together.

Reference case optimization

Fig. 4 shows the annual heat flow profiles (top plot) in the reference case (described in Section 2.1), together with the evolution of the state of charge (SoC) of the STES unit (bottom plot). In the SoC diagram, it is clear that the initial and final state are equal. It is interesting to observe that during spring, most of the heat demand is provided by the backup heating plant, while the storage tank is left nearly empty. In summer, the backup plant is switched off and the solar collectors provide most of the heat demand, while at the same time charging the storage tank. In early autumn, the solar energy

stored in the storage tank is used, but around October the backup heater is switched on at maximum power. The surplus heat is stored in the STES and used to bridge the demand peaks of the cold season.

A similar pattern is seen in the reduced problem results. The shape of the SoC trajectory is comparable to that of the full year optimization, albeit shifted in time. This time shift has no importance because of the periodic boundary conditions. Again, we can discern a spring period during which the backup plant supplies most of the heat demand, a summer period during which the backup is not used and surplus solar energy is stored for later use, and a winter period during which the backup plant is continuously at nominal power and where the storage is generally in discharge mode. The maximum SoC for both optimization problems is similar.

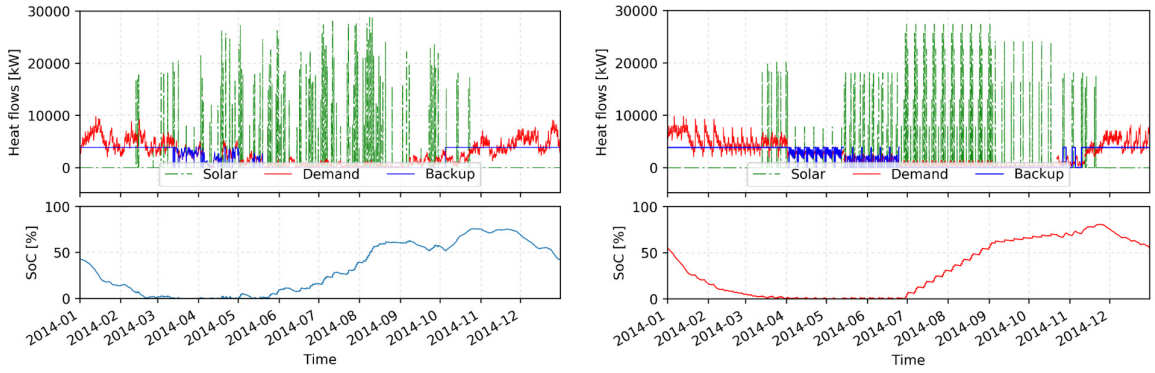

Fig. 4. Reference results with heat flows and state of charge of STES. Left: full optimization. Right: reduced optimization based on 12 representative weeks.

In this case, a total of 17.14 GWh of backup energy is used in one year. 6.51 GWh of solar energy is injected into the node, of which 1.12 GWh is lost due to heat losses of the storage tank. Combined they correspond to the 22.53 GWh annual heat demand of the neighbourhood. For this configuration, no solar energy is curtailed. In comparison, in the reduced model 17.19 GWh of backup energy is used, 6.58 GWh of solar energy and 1.12 GWh of energy is lost during storage.

3.2. Parameter sweep

In this section it is checked how well the optimization with representative periods represents the actual solution. Besides the reference design, some variations in the **volume of the storage tank (V)**, the **solar collector area (A)** and the **backup nominal power (P)** are considered.[4] The aim of this variation is twofold: the first is to check whether the variation in the total required annual backup energy is comparable for the full optimization and the reduced problem; the second is to check whether designs that are infeasible in the full optimization are also infeasible in the reduced problem. A total of 80 parameter combinations (4 x 4 x 5) is calculated. In addition, several scenarios for the selection of representative weeks are considered: between 6 and 12 three-day-periods and weeks are selected according to the optimization problem described in Section 2.1.

Fig. 5 shows an overview of the parameter variation study for the reduced optimization with 12 representative weeks. The four subplots show results for different values of the solar collector area A, the coloured markers indicate the storage volume V, and different points with the same marker and colour have different nominal backup power P.[5] On each of the x-axes, the full year total backup annual energy use (AEU) is shown, whereas the y-axes show the total backup AEU for the representative weeks optimization.

[4] V ∈ {50000, 75000, **100000**, 125000} m^3, A ∈ {20000, 40000, **60000**, 80000} m^2, P ∈ {3.6e6, **3.85e6**, 4.1e6, 4.35e6, 4.6e6} W, reference case parameters in bold

[5] For the same A and V, the backup energy needed decreases with increasing P: the lower the nominal power, the more the system must rely on the storage tank to bridge high demand peaks, and the more heat is lost from the tank.

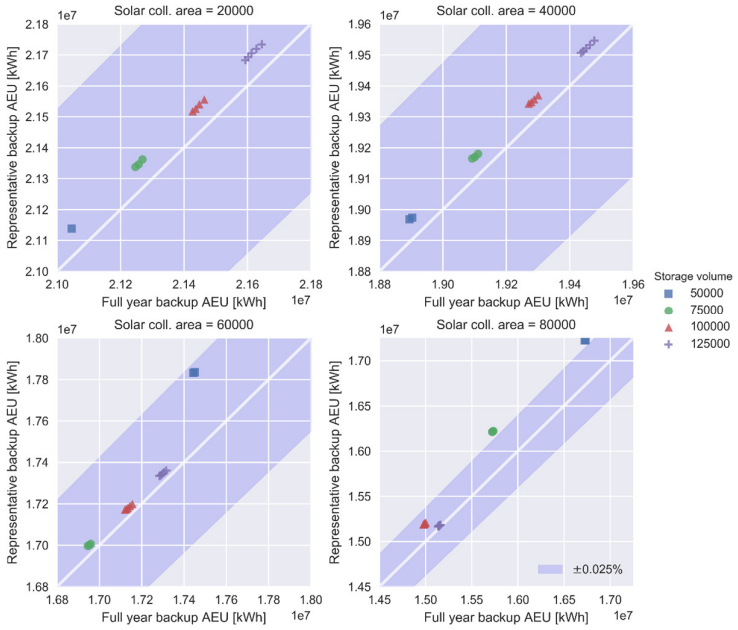

*Fig. 5. Parameter sweep of **12 representative weeks** optimization compared to full year optimization. The blue band shows a ±2.5% accuracy band around the line of equal annual energy use (AEU) for both optimization problems.*

In addition, the $x = y$ bisector is highlighted in all subplots: in an ideal case, all results would lie on this line, indicating a perfect representation in the reduced problem. Clearly, this is not always the case, however most solutions fall within a ±2.5 % error margin as indicated by the blue shaded area. Be aware that the four subplots do not show the same range or scale on their axes; this is to better interpret results that lie close to one another. The yearly energy need clearly decreases with an increasing solar collector area A. The fact that most results in Fig. 5 lie more or less on a straight line with the same slope as the bisector is positive: this means that when we compare two designs in either the full year optimization or the reduced optimization, they will have the same order from the viewpoint of the energy objective.

Digging deeper into the results, we see clear groups based on the value of the storage volume. The different results within each group vary in nominal backup power, but this seems to be only a minor variation. This seems logical, since for the same values of V and A, the backup energy required will be largely the same. As such, the nominal power only determines whether the optimization problem is feasible or not. Furthermore, when results seem to "jump out" of the trend of most results, this is due to a misrepresentation of the curtailment in the solar collector.

Fig. 6 shows results of the analysis with 8 representative three-day periods. These results are similar to the ones in Fig. 5, although the deviation is sometimes larger, sometimes smaller than for the weekly time periods. However, the cases with 60 000 and 80 000 m^2 solar collector area display an *inversion* of the results, i.e. the order of the results in terms of backup energy needed is not always the same for the full optimization and the reduced problem. This can prove problematic, since in an evolutionary algorithm, this means that the reduced problem could lead to a different optimum than the full optimization.

Fig. 7 shows the results for 6 representative three-day periods. Here the relative deviation from the bisector is much higher. Deviations in both positive and negative sense are possible, and the cause of this problem is to be sought in an erroneous representation of the combination of heat demand and solar collector production profiles during summer.

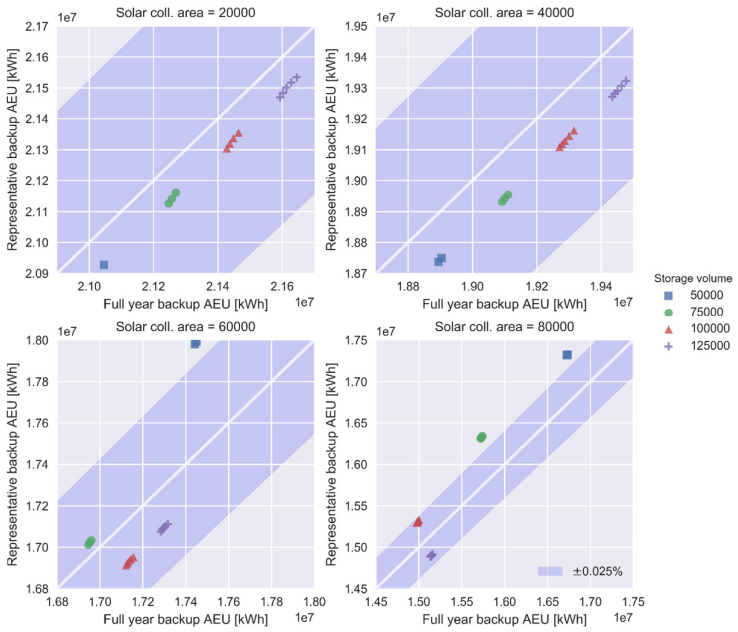

*Fig. 6. Parameter sweep of **8 representative three-day periods** optimization compared to full year optimization. The blue band shows a ±2.5% accuracy band around the line of equal yearly energy use for both optimization problems.*

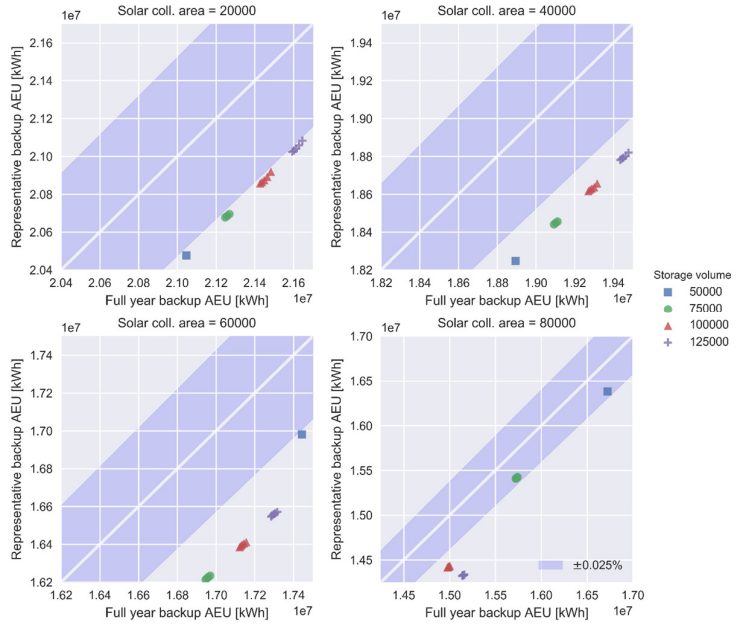

*Fig. 7. Parameter sweep of **6 representative three-day periods** optimization compared to full year optimization. The blue band shows a ±2.5% accuracy band around the line of equal yearly energy use for both optimization problems.*

3.3. Calculation time reduction

Fig. 8 shows a comparison of the calculation time for the full optimization and for the various numbers of representative time periods used. Each boxplot summarizes the results for 80 runs, corresponding to the parameter sweep described in the previous section. The calculation time is measured between the start of the compilation of the model equations and the end of the solution process. These results were compared on a Dell Latitude E7470 device with an Intel® Core™ i7-6600U 2.60 GHz with 2 cores (4 logical processors); the device has 16 GB RAM and runs Windows 10 as operating system. On average, the compilation and solution is sped-up by a factor of between 4.8 and 6.1 for representative weeks and between 5.7 and 7.7 for the three-day representative periods.

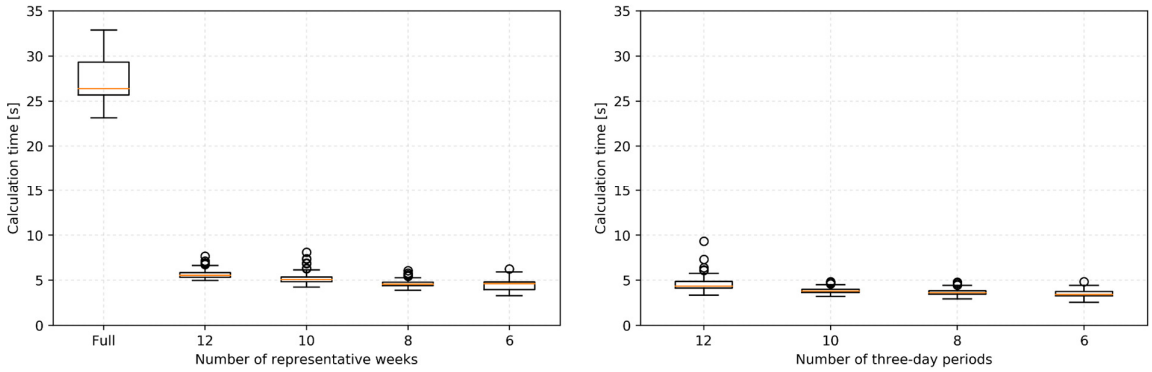

Fig. 8. Calculation time statistics for different numbers of representative weeks and full optimization (left) and for representative three-day periods (right).

4. Discussion

Although the results of the reduced optimization accurately represent the value of the optimal objective for the full year optimization in most cases presented in Section 3.2, the curtailment of the solar collectors' output in cases with high solar collector area and limited storage volume causes differences in the annual backup energy needed. It seems that for the majority of the year, the accuracy of the time profiles based on representative time periods is sufficient, but during the summer, errors due to a misalignment of the low heat demand and high solar collector output can accumulate quickly, leading to a much higher or lower curtailment than in the full year optimization.

A possible solution would be to change the way summer weeks are selected in the representative time period optimization. Potential strategies include simply selecting more summer weeks, applying additional requirements for the correlation between solar output and heat demand, or using longer representative time periods during summer. In the worst case, a full optimization will still be needed for the summer months, but given the results in Section 3.3, this will still be faster than the actual full year optimization. One way to implement this would be to first run a heavily reduced optimization to explore the year, select the period where the backup plant is completely shut down and run the full optimization only for this part of the year, while using representative time periods for the rest.

Another aspect to consider is whether or not these problematic optimization results are fully relevant. Obviously, from an energy point of view they are; but in a later stage, where investment and running cost are considered as well, cases where a lot of solar curtailment occurs will probably not be optimal, since either the storage tank is too small or the solar collector area too large, leading to cost inefficiencies. Still, since there are also cases where the reduced optimization shows less curtailment than in the full optimization, this is not (yet) an argument to completely disregard the issues with curtailment, and further investigation is needed.

An additional issue that has been found is that currently, more than half of the calculation time is needed for compilation. Since the problem structure is similar during the parameter sweep, additional speed-up would be obtained if this similarity could be employed.

5. Conclusions and further work

A reference case of a thermal system with a neighbourhood representing a specific heat demand profile, a solar thermal collector array, a seasonal storage tank and a backup heating plant, in which the heat flows are optimized with respect to minimum annual energy use of the backup plant has been presented. The novelty is the combination of an optimization-based selection procedure for representative time-slices with a control optimization of a seasonal thermal energy storage system, and the comparison of the obtained results with those of the full year optimization.

This study has shown that there is potential for using reduced optimization formulations with representative time periods to approximate the objective function of the full year optimization with a

high degree of accuracy. A substantial calculation time reduction is possible, of course depending on the number of selected representative time slices, but for the cases studied here exceeding a speed-up factor of 4.8 to 7.7. The charging and discharging behaviour of the reduced problem are similar to that of the full year optimization in most cases.

However, difficulties to represent curtailment of solar thermal collector power in cases with a higher ratio of solar collector area compared to storage volume were identified for a limited number of cases. Further study is needed to see how else these problems can be solved. More future steps to be taken are to use this strategy in combined control and design optimization of a larger scale energy system, to add investment and running cost to the optimization and to test this strategy with a mixed integer linear programming (MILP) optimization problem.

Acknowledgement

The authors gratefully acknowledge the financial support for this work by the European Union, the European Regional Development Fund ERDF, Flanders Innovation & Entrepreneurship and the Province of Limburg through the project 'Towards a Sustainable Energy Supply in Cities'. Furthermore, VITO is gratefully acknowledged for the financial support of Bram van der Heijde, Luca Scapino and Annelies Vandermeulen through a PhD Fellowship.

References

[1] A. Vandermeulen, B. van der Heijde, D. Patteeuw, D. Vanhoudt, R. Salenbien, and L. Helsen, "modesto - a Multi-Objective District Energy Systems Toolbox for Optimization," in *5th International Solar District Heating Conference*, 2018.

[2] P. Nahmmacher, E. Schmid, L. Hirth, and B. Knopf, "Carpe diem: A novel approach to select representative days for long-term power system modeling," *Energy*, vol. 112, pp. 430–442, 2016.

[3] K. Poncelet, H. Höschle, E. Delarue, A. Virag, and W. D'haeseleer, "Selecting Representative Days for Capturing the Implications of Integrating Intermittent Renewables in Generation Expansion Planning Problems," *IEEE Trans. Power Syst.*, vol. 32, no. 3, pp. 1936–1948, 2017.

[4] D. Patteeuw and L. Helsen, "Combined design and control optimization of residential heating systems in a smart-grid context," *Energy Build.*, vol. 133, pp. 640–657, 2016.

[5] J. Timmerman, M. Hennen, A. Bardow, P. Lodewijks, L. Vandevelde, and G. Van Eetvelde, "Towards low carbon business park energy systems: A holistic techno-economic optimisation model," *Energy*, vol. 125, pp. 747–770, Apr. 2017.

[6] M. Welsch, M. Howells, M. Bazilian, J. F. DeCarolis, S. Hermann, and H. H. Rogner, "Modelling elements of Smart Grids - Enhancing the OSeMOSYS (Open Source Energy Modelling System) code," *Energy*, vol. 46, no. 1, pp. 337–350, 2012.

[7] PlanEnergi, "Summary technical description of the SUNSTORE 4 plant in Marstal." [Online]. Available: http://www.solarmarstal.dk/media/2854117/summary-technical-description-marstal.pdf. [Accessed: 15-Jan-2016].

[8] T. Pauschinger and T. Schmidt, "Solar unterstützte Kraft-Wärme-Kopplung mit saisonalem Wärmespeicher," *Euro Heat & Power*, 2013.

[9] W. Hart, C. Laird, J. Watson, D. Woodruff, G. Hackebeil, B. Nicholson and J. Siirola, *Pyomo - optimization modeling in python*, Second., vol. 67. Springer Science & Business Media, 2017.

[10] Gurobi Optimization Inc., "Gurobi Optimizer Reference Manual." 2016.

[11] J. Vandewalle and W. D'haeseleer, "The impact of small scale cogeneration on the gas demand at distribution level," *Energy Convers. Manag.*, vol. 78, pp. 137–150, Feb. 2014.

[12] R. Baetens, R. De Coninck, F. Jorissen, D. Picard, L. Helsen, and D. Saelens, "OpenIDEAS – an Open Framework for Integrated District Energy Simulations," *BS2015, 14th Conf. Int.*

Build. Perform. Simul. Assoc., pp. 347–354, 2015.

[13] M. Wetter, W. Zuo, T. S. Nouidui, and X. Pang, "Modelica Buildings library," *J. Build. Perform. Simul.*, vol. 102, no. 1, pp. 253–270, 2014.

[14] I. De Jaeger, G. Reynders, and D. Saelens, "Impact of spatial accuracy on district energy simulations," *Energy Procedia*, vol. 132, pp. 561–566, 2017.

[15] R. Baetens and D. Saelens, "Modelling uncertainty in district energy simulations by stochastic residential occupant behaviour," *J. Build. Perform. Simul.*, vol. 9, no. 4, pp. 431–447, Jul. 2016.

[16] B. van der Heijde, A. Vandermeulen, D. Patteeuw, R. Salenbien, and L. Helsen, "Optimizing thermal energy storage in 4GDH," in *3rd International Conference on Smart Energy Systems and 4th Generation District Heating*, 2017, no. September.

[17] H. Gadd and S. Werner, "Daily heat load variations in Swedish district heating systems," *Appl. Energy*, vol. 106, pp. 47–55, Jun. 2013.

[18] J. Timmerman, "Development of a Techno-Economic Energy Model for Low Carbon Business Parks," University of Ghent, Belgium, 2015.